Engineered Science

RESEARCH PAPER View Article Online

Fabrication of Nano-Patterned Arrays Using Pulsed Light Technique

Ilwoo Seok[1*], Aktaruzzaman Al-Hossain[2], Mohammad Waliullah[3] and Jong Eun Ryu[4]

Pulsed light aided thin film de-wetting process to fabricate nano-patterned array is introduced. Being compared to thermal annealing process, highly intense pulsed light with millisecond duration plays a role to transform solid-state thin-film to metastable and provides enough energy as a driving force to form island-like pattern. Topological analysis using SEM and AFM was performed to confirm fabricated structures. In addition, optical performance regarding surface-plasmon resonance and light absorption was studied by experimental UV-VIS spectroscopy and computer aided electromagnetics (EM) simulation. This research will benefit to the real-time roll-to-roll fabrication for the fabrication of nanostructures without using of thermal soaking and vacuum process.

Keywords: Dewetting; Nanostructure; Pulsed-light

Received 13 February 2019**, Accepted** 15 April 2019

DOI: 10.30919/es8d506

1. Introduction

Today is the booming era of nanotechnology- one might say. More than one thousand registered nanotechnology-based commercial products were available on the global market in 2009.[1] Now it is 2017. New frontiers of technology are being achieved and more and more researchers are getting involved in this field. Among these technologies, the field of periodic patterns of nanoparticles is growing in relevance.

It has proved its usefulness in the fields of Photovoltaics and Immunoassay.[2-4] Currently, the authors of this paper are involved in a project using this technology to build a DNA identification device, although, that is out of the scope of this paper. However, these are only a few among many applications of nanoparticle patterns. In the future, it may give birth to hundreds of new inventions. Who knows the limits to the opportunities? So let us delve deeper into this vast, wonderful technology.

A nanoparticle pattern contains thousands of nanoparticles separated from each other at a specified distance. To create a pattern, there are two approaches: bottom-up and top-down.[5] In bottom-up approach, individual nanoparticles are obtained first, and then some reagents are used to prevent them to agglomerate. In top-down approach, which is the scope of this research, a thin film is created first by sputtering or evaporation. Then nanoparticles are segregated. In terms of Fluid Mechanics, this segregation process is called dewetting.[6,7]

[1] *Department of Mechanical Engineering, Arkansas State University, AR 72401, USA*

[2] *Department of Mechanical Engineering, Stony Brook University, NY 11790, USA*

[3] *Department of Mechanical Engineering, The University of Texas at Dallas, TX 75080, USA*

[4] *Department of Mechanical and Aerospace Engineering, North Carolina State University, Raleigh, NC 27695, USA*

***E-mail:** iseok@astate.edu*

Dewetting involves applications of heat on a deposited thin film. The temperature required to segregate nanoparticles depends on the motion of the atoms, which is far below the melting temperature of the deposited film. A pre-existing hole or film edge is the starting point of forming the pattern of nanoparticles. The pattern is visually similar to the separation of islands, hence the nomenclature of this pattern as nano-islands. The nano-island formation is dependent on the thickness of the deposited film, which can be controlled from the beginning of fabrication. The surface energy reduction destabilizes the deposited thin film, leading to dewetting.

The limitations of these conventional techniques inspires many this research team to investigate for an alternative method to fabricate the periodic pattern. Top-down processes, like electron irradiation and ion irradiation, are limited due to the high expenses to buy and operate the machines. Restricted applications, along with the requirement of special training to operate the machines, are additional drawbacks. To create a pattern on the substrate by the use of conventional techniques is a time demanding process. Some researchers may use nano-imprint lithography for fabrication.[8] Suh and Lee, however, discovered that the NIL technique also includes problems related to mold feature distortion.[9] Low contrast between the polymer precursor and the master, along with the complexity to transfer patterns for molding and embossing techniques were additional problems that were reported.

A new approach using pulsed light heat treatment is being proposed in this paper to overcome the drawbacks of the existing technologies. This technique requires less sample preparation to generate arrays of nanoparticles.[10] It is a non-lithographic process[11] which removes the pattern deformation issues during masking and thin film contact. Furthermore, pulsed light technique is a less time consuming process to facilitate mass fabrication. The equipment and tools required for this technique are also much easier to operate. The production and technology purchasing for pulsed light technique are more cost effective than lithography due to the pre-mentioned corresponding benefits.[12–15]

It involves applying heat to the thin film by delivering high

intensity polychromatic light from a flash lamp. The flash lamp emits a wide range of wavelengths by converting electrical energy to light energy. This conversion of energy happens by storing electrical energy in a capacitor and passing charges to the Xenon gas-filled lamp.[12] Pulses of high intensity light are then emitted through the pulsed light hand piece crystal. The light energy is emitted on top of the thin film deposited on a substrate as shown in Fig. 1.

When the light energy hits the thin film, the film absorbs the light energy and converts it into heat energy. Heat is transferred from the top surface to the bottom of the thin film layer. The distribution of heat on the film surface is along the direction of the sapphire crystal. As the size of the crystal is decreased, the scattering effect is minimized. The technique is controlled by pulse and delay times. It emits high intensity light for a very short period of time. One light emission is called a pulse, and the time span for this emission is called a pulse time. A short interval between two pulses allows the thin film to maintain a steady temperature. This interval is called a delay or delay time. Several pulses and delays make a single shot, and there might be a longer time period between two shots, which is called a shot interval. All of these are shown in Fig. 2. The energy in the process is quantified in Joule per square centimeter area.

Because of their vulnerability to a phenomenon called surface plasmon resonance (SPR)[16,17] silver (Ag), gold (Au) and copper (Cu) were the materials of interest for fabricating these nano-island arrays. When light is incident upon a surface of any of these materials, some light is absorbed by the surface conduction electrons. It occurs when the frequency of incident photons matches the natural frequency of those electrons. As a result, they begin to oscillate in resonance at the interface of the substrate and coating material against the restoring force of positive nuclei. In terms of Quantum Mechanics, this oscillation is termed as surface plasmon, and, hence, the name surface plasmon resonance emerged. This phenomenon has helped to investigate the effectiveness of the pulsed light technique.

2. Experimental Methods

2.1 Thin Film Deposition and Nanoparticle Pattern Formation

A sputtering machine (Cressington Sputter Coater, 108) was used to deposit silver (Ag), gold (Au) and copper (Cu), separately, on top of several glass substrates. Prior to the thin film deposition, the glass substrates were cleaned using both acetone and de-ionized water. Sonication, along with acetone, was also used to clean the glass substrates. Sonication is the act of applying sound energy at high frequencies to agitate alien particles upon substrates facilitating their removal. The substrates were then dried by blowing nitrogen gas across the surface to ensure the removal of liquid particles. This introduced an inert layer on top of the substrates. The sputtering time was altered to deposit different thicknesses of thin film on the substrates. The longer the sputtering time, the thicker the layer of thin film. Deposition was performed at a 15 mA current flow with three different time settings of 30, 60 and 90 seconds. Cu is prone to surrounding gas contaminants. So, it was necessary to increase the deposition rate. For Cu, the current flow was set to 30 mA since the deposition was negligible for 15 mA.

2.2 Nano-island Array Formation

For dewetting, the annealing process was compared with the pulsed light technique. A long duration of the annealing process was required for dewetting of the thin film. A benchtop muffle (Muffle, Thermo Scientific) was used to anneal the deposited thin film. For Ag samples, which had deposition times of 60 and 90 seconds, a temperature of 400°C was applied for a duration of one hour to heat the film. For the rest of the samples, annealing was applied separately at a temperature of 300°C for a duration of one and a half hours. After analyzing the samples of the three materials, an additional annealing was applied at 400 °C for half an hour. The remaining annealing was applied for Au (60 sec and 90 sec), Ag (90 sec), and Cu (30 sec, 60 sec, and 90 sec) samples. Two Ag (60 sec and 90 sec) samples were also prepared applying an annealing temperature of 400 °C for half an hour. The annealing had been performed without a vacuum in the furnace. To compare annealing with the pulsed light technique, the Ag film was shot by pulsed light to provide heat energy, where each shot had a combination of five pulses and five delays. A time span of 20 milliseconds was set for each pulse and delay. Three and six shots were provided separately on top of the film with the energy of 40 J/cm^2. The time gap between two consecutive shots was one second. Pulsed light shots were applied for the Ag (60 sec and 90 sec) samples.

2.3 Optical Property Evaluation

A UV/VIS Spectrometer (Perkin Elmer, Lambda 35) was used to examine the optical properties of the fabricated periodic pattern, which depends on the size and distribution of the nanoparticles. Wide range wavelengths of electromagnetic radiation were applied to the samples. Transmission tests of the samples were conducted at a scan rate of 240 nm/min. The range of wavelengths for each test was 200 to 700 nm.

2.4 Surface Morphology Investigation

To investigate the surface morphology after the heat treatments, a scanning electron microscope (SEM) was used. Prior to this imaging of the samples, an additional sputtering of gold (Au) on top of all the samples was added to make the samples' surface conductive. A

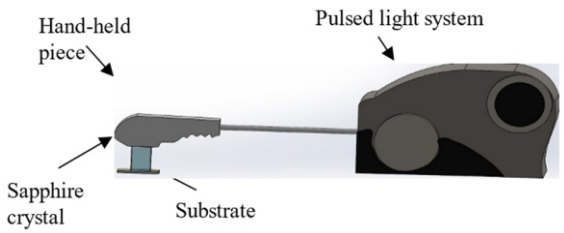

Fig. 1 Pulsed light system for thin-film dewetting process.

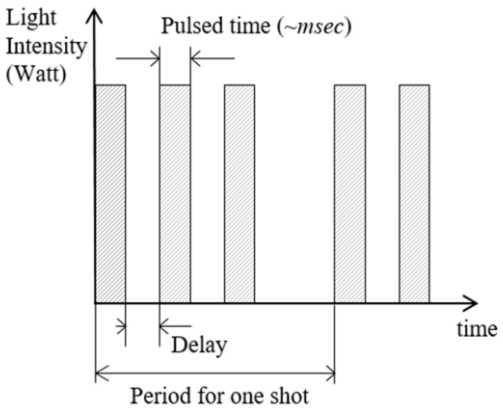

Fig. 2 Pulsed light profile with short time duration in milliseconds.

magnification of 40,000X was applied with a high voltage of 10.0 kV to view the images of the dewetted thin film. The size and shape of the nanoparticles were determined. It was then possible to form a relationship between the results of the UV/VIS spectrometer and SEM.

2.5 Simulation Work

A simulation using COMSOL was run to grasp a better understanding of what was happening during the surface morphology investigation. The results of simulation revealed an interesting relation between the transmission spectrum of silver and formation of electromagnetic field cloud in between the nanoparticles. The geometry of the simulation was defined as a rectangle with a circle at the center. Surrounding the circle, there were uniformly distributed half-circles and quadrants in the boundary region of the rectangle. Obviously, the rectangle represents a small part of the glass substrate focusing on a single nanoparticle, for example, the circle at the center. The half-circles and quadrants represent other nanoparticles surrounding the single nanoparticle in focus. The material for the glass substrate was defined as quartz. The material properties for electro-magnetic simulation are given; electrical conductivity ($\sigma = 10^{-11}$ S/m), relative permittivity ($\varepsilon_r = 4.7$), and relative permeability ($\mu_r = 1$). Although the latter two properties are dependent upon the frequency of the incident light, they do not vary much in case of glass substrate.

For silver, thermal conductivity, resistivity, coefficient of thermal expansion, heat capacity at constant pressure, density, Young's modulus, Poisson's ratio, bulk modulus, and shear modulus were defined as piecewise inputs – all as functions of temperature. Electrical conductivity was considered to have a fixed value of 6.3 (10^7) S/m. Due to large variations depending upon the wavelength of incident light, relative permittivity and relative permeability were defined as interpolation functions. The input values for the latter two were taken from the data provided by Johnson and Christy for optical constants of noble metals.

The goal of the simulation was to see how different wavelengths of light, for example, different amounts of photon energy, interact with the surface electrons in the conduction band. It was assumed that if SPR occurs, the plasmon would create a strong, uniform electric field in between the nanoparticles.[18] This is also backed by the nanoparticles' similarity in uniform distribution. To verify the assumption, the relations between relative permittivity, relative permeability, conductivity, and electric field were defined by the wave equation that follows.

$$\nabla \times \mu_r^{-1} (\nabla \times \vec{E}) - \kappa_0^2 \left(\varepsilon_r - \frac{\sigma \vec{J}}{\omega \varepsilon_0} \right) \vec{E} = 0$$

A perfect electric conductor was assumed and expressed by the following equation.

$$\vec{n} \times \vec{E} = 0$$

Because the direction of the electric field must be normal to the surface, an initial value of "1" was assigned for only the z-component of the electric field, while the x- and y-components were assigned to be zero.

3. Results and discussion

3.1 Observation of Surface Plasmon Resonance of annealed samples

Fig. 3 presents the transmission spectra of all the samples for the 60 second deposition. It reveals that the Au sample has a valley at approximately 560 nm. This valley corresponds to where light wavelengths were absorbed the most. It also shows that Ag shows a start of a formation of a peak in transmission at 460nm, while Cu shows no sign of response with incoming wavelengths.

Due to the increased increment of both annealing temperature and thickness, the sizes of the nanoparticles that were formed also increased. An increase in the diameter of the nanoparticle size also increased the distance of the charges between the opposite sides of the particle, which in turn reduced the restoring force. This restoring force reduction has led to the shift of the plasmon resonance wavelength. The resonance peak for Au was shifted to 568 nm. The same trend is observable for the Ag sample, where the transmission valley is at approximately 460 nm. Ag had no peak resonance with a deposition time of 30 seconds because the deposition was so thin that it couldn't handle the high temperature that was applied.

Further examination continued to check the relation between surface plasmon resonance and thickness of the deposited film. Higher deposition times of the materials yielded greater thicknesses of the films. Higher thickness of the film contributes to both larger average particle diameter and also higher dewetting temperatures needed for annealing as shown in Fig. 4.

3.2 Comparison with Pulsed Light Dewetting with thermal

After thorough investigation of the effect of various materials on surface plasmon resonance, the viability of pulsed light was checked for the thin film of Ag. Ag was chosen as the material for the pulsed light application because it has probably the greatest possibility to allow plasmon resonance. Ag, as a noble material, possesses lower d-electron energy in the conduction band. Additionally, Ag has lower adhesion energy which allows dewetting to occur deliberately. That is why it is the chosen material for this test. Since Ag (30 sec) showed no significant peak, 60 second second deposition samples was taken to work with. These samples were compared with two types of pulsed light dewetted samples – 3 shots and 6 shots. 3 shot sample seems to have no valley of transmission, while 6 shots resembles the sample annealed for half an hour.

Fig. 4 confirms that 3 shots could not provide the energy necessary to tear the film up and segregate the nanoparticles. In other words, the heat energy converted from the provided light energy could not penetrate the film to initiate the dewetting process. In mathematical terms, the surface energy of the glass substrate is greater than the summation of energy of the island-substrate interface and the film. To dewet a film, the energy of the substrate must be less than the sum of

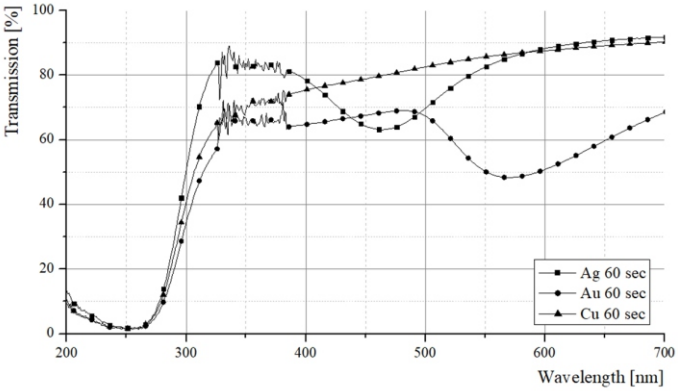

Fig. 3 Transmission spectra for Ag, Au and Cu samples (deposition times 60 sec). Annealing temperature for the all samples was 300 °C for time duration of 1.5 hours. An additional temperature of 400 °C was also done for Au sample for half an hour.

the other two energies just mentioned. In the case of the 6 shots, it proves itself as an equivalent of annealing process. So it might be considered as a good alternative for annealing, saving time and, hence, production cost of nanoparticle patterns.

3.4 Findings from Electro-Magnetic Simulation and Light Absorption Study

The results of the simulation confirmed our initial assumption that SPR creates a strong and uniform electric field. It showed that the strongest and most uniform electric field was created at the frequency corresponding to the same value of the wavelength where the peak of the transmission occurs.

Fig. 7 shows that the electric field is not uniformly developed yet at 300nm – confirmed accordingly in Fig. 5 as the curve is flat. At 442 nm, strong and uniform electric fields is generated in between the nanoparticles. UV/VIS spectroscopy and also revealed that a transmission peak right after 450 nm exists. Wavelength of 442 nm is close to 450 nm; that validates the initial assumption that the plasmon creates a strong and uniform electric field when SPR occurs. For 613 nm and 800 nm, the figure shows that a uniform electric field is still there, though faded in strength. It corresponds to the UV/VIS plot where the transmission curve already went up. The comparison between the contour plots of COMSOL simulation and the UV/VIS plots indicate a relation between the amount of electric field generated and the amount of light transmitted or absorbed by the nanoparticles. Further investigation can be carried out to find an analytical or empirical relation between these two parameters.

Fig. 8 shows the result of light absorption study using simulation. Specifically incoming light of wavelengths ranging from 450 to 500nm has a valley in transmission curve and means to be absorbed. It is coincident to the experimental results shown in Fig. 4 as both curves have a peak of valleys around 475 nm. The experiential's curve is wider than simulation's one due to the non-uniformity in islands size and gaps. Trapped lights are observed in contour plot (left bottom in Fig. 8).

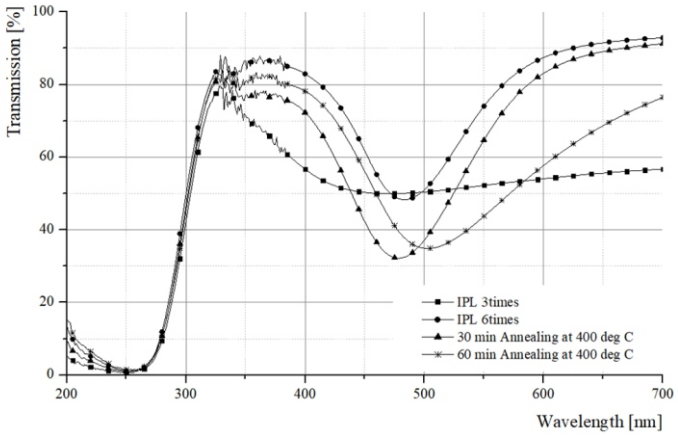

Fig. 4 Comparison of transmission spectra for silver thin-film of 60 sec deposition with intense-pulsed light and thermal annealing at 400 °C.

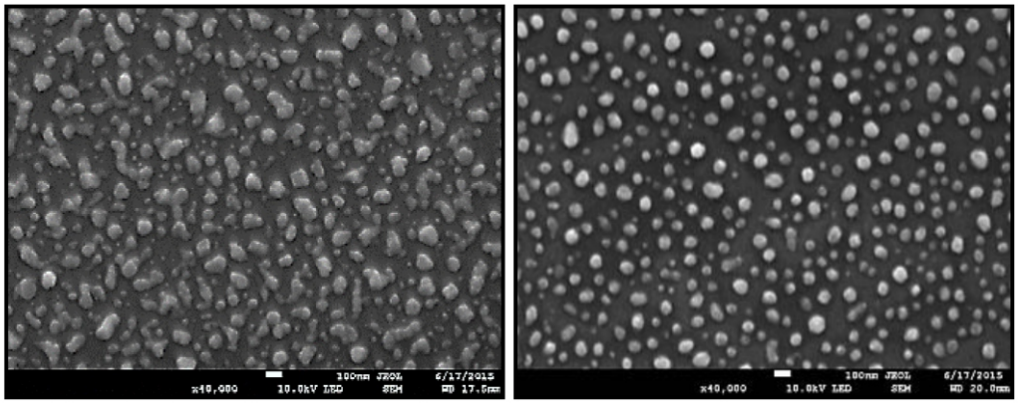

Fig. 5 Scanning electron microscope image of Ag nanoparticles formed by 3 pulsed light shots (left) and 6 shots (right), respectively.

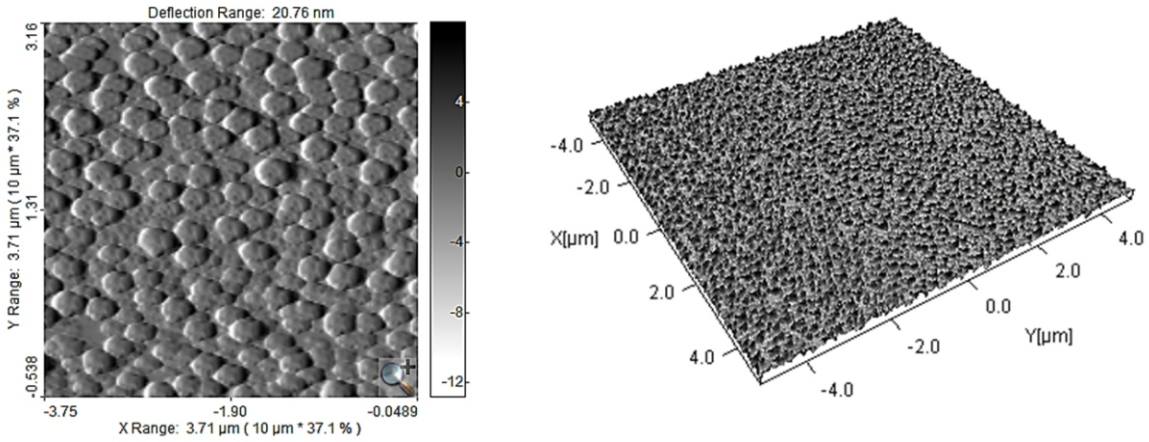

Fig. 6 Atomic force microscope image showing the Ag nano-patterned array onto the SiO_2 substrate.

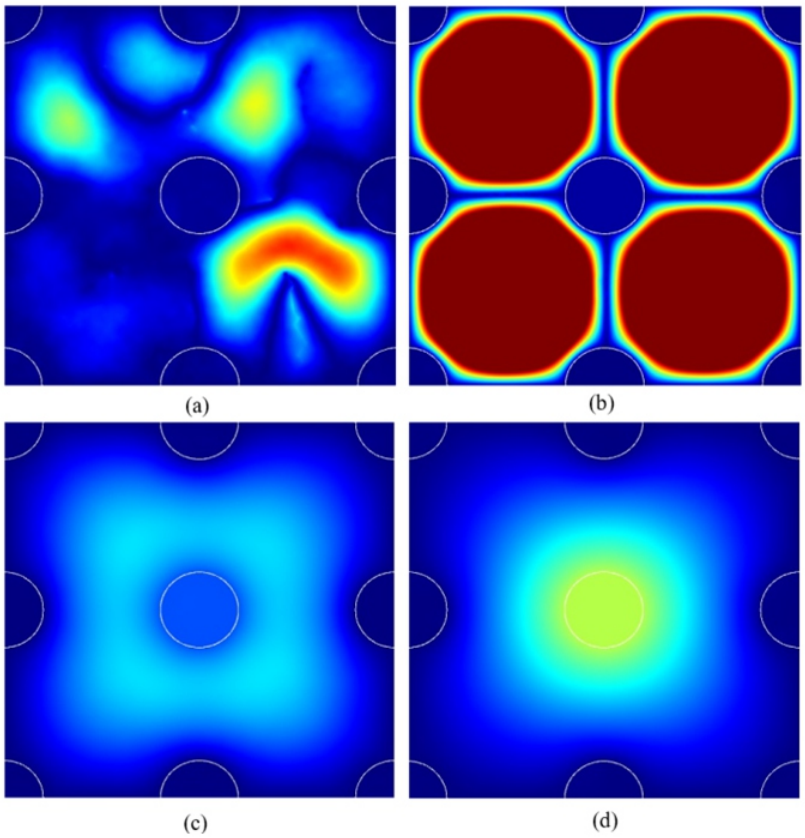

Fig. 7 Electromagnetic filed contour plots for (a) 300 nm, (b) 442 nm, (c) 613nm, and (d) 800nm.

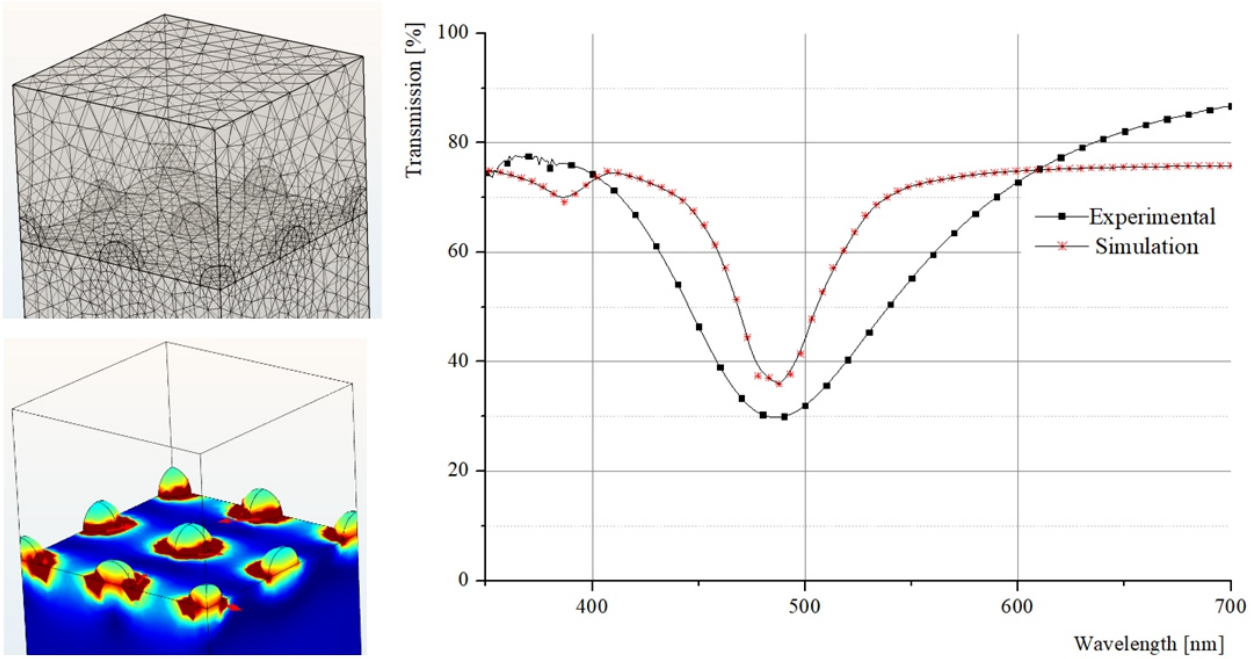

Fig. 8 Finite element model and its electric field at 475 nm and comparison of transmission profiles of nano-island structures between experiment and simulation.

4. Conclusions

During this experiment, the viability of pulsed light heat treatment as a new approach for nano-patterns, which is comparable to the annealed process, has been studied. It has been found that the formation of nanoparticle patterns is largely dependent on thin film thickness as well as energy and time exposure of intense pulsed light to the deposited film. Moreover, the transformation of wavelengths is related to the decrease of surface energy of the substrates, which increases the transportation of the materials. Furthermore, various noble materials transformed the wavelengths in different regions of the spectrum, while all being treated with the same parameters. Overall, it has been found that the deposited thin film thickness and the types of noble materials have a large impact on the optical properties. The ease of operation and the time reduction of the pulsed light process over the comparable conventional fabrication processes create an alternative solution for nanoparticle fabrication. This new alternative can create a wide range of new applications in photonics and surface treatment.

Conflict of interest

There are no conflicts to declare.

Acknowledgements

This work was supported by Major Research Instrument program from the National Science Foundation (Grant number: CMMI-1229404). In addition, support has been provided in part by the Arkansas Biosciences Institute, the major research component of the Arkansas Tobacco Settlement Proceeds Act of 2000.

References

1. M. J. Madou, *Manufacturing Techniques for Microfabrication and Nanotechnology*. CRC Press, 2011.
2. I. Seok, J. Falls, and S. Haran, presented at the SPIE Smart Structures and Materials + Nondestructive Evaluation and Health Monitoring, San Diego, California, USA, 2013, 86910K.
3. P. Spinelli, *J. Opt.*, 2012, **14**, 024002.
4. J. W. Menezes, J. Ferreira, M. J. L. Santos, L. Cescato, and A. G. Brolo, *Adv. Funct. Mater.*, 2010, **20**, 3918–3924.
5. A. Biswas, I. S. Bayer, A. S. Biris, T. Wang, E. Dervishi, and F. Faupel, *Adv. Colloid Interface Sci.*, 2012, **170**, 2–27.
6. C. V. Thompson, *Annu. Rev. Mater. Res.*, 2012, **42**, 399–434.
7. J. Becker *et al.*, *Nat. Mater.*, 2003, **2**, 59–63.
8. L. J. Guo, *Adv. Mater.*, 2007, **19**, 495–513.
9. Y. S. Kim, K. Y. Suh, and H. H. Lee, *Appl. Phys. Lett.*,2001, **79**, 2285–2287.
10. J. Bischof, D. Scherer, S. Herminghaus, and P. Leiderer, *Phys. Rev. Lett.*, 1996, 77, 1536–1539.
11. T. Ito and S. Okazaki, *Nature*, 2000, **406**, 1027.
12. N. L. Schoenewolf, M. J. Barysch, and R. Dummer, *Basics Dermatol. Laser Appl.*, 2011, **42**, 166–172.
13. J. Ryu, K. Kim, H. S. Kim, H. T. Hahn, and D. Lashmore, *Biosens. Bioelectron.*, 2010, **26**, 602–607.
14. H. S. Kim, S. R. Dhage, D. E. Shim, and H. T. Hahn, *Appl. Phys. A*, 2009, **97**, 791.
15. R. Dharmadasa, M. Jha, D. A. Amos, and T. Druffel, *ACS Appl. Mater. Interfaces*, 2013, **5**, 13227–13234.
16. K. A. Willets and R. P. Van Duyne, *Annu. Rev. Phys. Chem.*, 2007, **58**, 267–297.
17. P. Pattnaik, *Appl. Biochem. Biotechnol.*, 2005, **126**, 79–92.
18. A. N. Grigorenko, N. W. Roberts, M. R. Dickinson, and Y. Zhang, *Nat. Photonics*, 2008, **2**, 365.

